ELSEVIER

Journal of Archaeological Science 33 (2006) 1651–1665

Journal of Archaeological SCIENCE

http://www.elsevier.com/locate/jas

Optically stimulated luminescence dating of Southern High Plains archaeological sites

James K. Feathers [a,*], Vance T. Holliday [b], David J. Meltzer [c]

[a] Department of Anthropology, University of Washington, Box 353100, Seattle, WA 98195-3100, USA
[b] Departments of Anthropology and Geosciences, University of Arizona, Tucson, AZ 84721-0030, USA
[c] Department of Anthropology, Southern Methodist University, Dallas, TX 75275-0336, USA

Received 16 November 2005; received in revised form 25 February 2006; accepted 27 February 2006

Abstract

The Southern High Plains of North America is rich in archaeological sites, but many are not well constrained chronologically, owing to a lack of material for radiocarbon dating. A program of optically stimulated luminescence (OSL) dating, applying mainly single-grain analyses, was therefore initiated. Many samples have independent age estimates from radiocarbon to check the OSL results, but OSL age estimates are also provided for those sites that otherwise lack secure chronological control. Sediment samples for OSL were obtained primarily from Paleoindian and Archaic localities, though include deposits of more recent age. Through the analysis of single grains, equivalent dose—the numerator of the age equation—is evaluated independently on numerous grains. The distribution of these values is relatively broad for some samples, and this is attributed to post-depositional mixing. Mixing is also evident in some samples with more narrow distributions. Selecting portions of the mixed distributions for age determination allows more accurate dating for some samples, but the nature of the distributions limits the resolution on others, conclusions that cannot be as easily drawn from multi-grain analysis. Where independent age control is available, most OSL results broadly conform; however, some samples show discrepancies that are not readily explained, but may relate to association or dose rate problems. This underscores the desirability of obtaining where possible suites of chronological evidence.

Keywords: Optically stimulated luminescence; Single-grain resolution; Southern High Plains; Paleoindian; Sediment turbation

1. Introduction

The Great Plains of North America has a rich archaeological record that spans the period from the Late Glacial to the Historic, a period of time that has also seen significant changes in climate, ecology, and human adaptations. Chronometric dating of archaeological sites in many areas of the Great Plains, however, is often problematic, largely because charcoal—the preferred material for radiocarbon dating—is scarce in this grassland environment with few trees. Lack of charcoal has meant reliance on carbon materials that carry greater uncertainties. Bone can be abundant in the archaeological and paleontological sites of interest, but often is not suitable for radiocarbon dating because of poor preservation of organic carbon. Radiocarbon dating of bulk organic matter from soils has been utilized, but the results are often problematic [29,30].

Recently, luminescence dating has been applied successfully to eolian sediments on sites of the Great Plains [9,11,45,46]. Luminescence analysis of sediments dates the last exposure to sufficient daylight, a burial event that provides a direct date of sediment deposition [1,2,6]. It is applicable to ubiquitous materials, mainly quartz and feldspars, which are abundant in this geological setting. Analytical complications can arise from post-depositional disturbance and from partial resetting (or bleaching) of sediment grains at the time of deposition. Therefore, much recent effort has focused on single-grain dating through the examination of age distributional

* Corresponding author.
E-mail addresses: jimf@u.washington.edu (J.K. Feathers), dmeltzer@smu.edu (D.J. Meltzer).

0305-4403/$ - see front matter © 2006 Elsevier Ltd. All rights reserved.
doi:10.1016/j.jas.2006.02.013

data among grains, allowing disturbance or partial bleaching to be detected.

In an effort to extend the application of this method, we initiated a program of optically stimulated luminescence (OSL) dating of various sediment types from archaeological sites on the Southern High Plains of western Texas and eastern New Mexico. This region is of longstanding interest for its particularly rich, but unevenly dated record of Late Glacial and Early Holocene Paleoindian occupations, as well as the evidence it provides of human adaptive responses to later (Middle Holocene) climate change.

Our goals, in sampling for OSL dating eight archaeological sites (some with multiple components) in this region, were threefold: to evaluate the utility of single-grain optically stimulated luminescence; to use sites in which components or occupations have accompanying radiocarbon ages as a check against the OSL results; and, to derive OSL ages from sites which at the moment lack any chronological control, except for general age estimates based on typology. Obviously, resolving the first two matters will help determine how much confidence can be placed in the results of the third.

2. Geological setting

The Southern High Plains is a semi-arid plateau of mixed prairie grasslands. The low relief surface is underlain by an extensive eolian deposit heavily modified by pedogenesis. Known as the Blackwater Draw Formation, this deposit accumulated episodically through the Pleistocene and forms the bedrock for the archaeological and other late Quaternary deposits of the region [18]. The only topographical relief on this otherwise flat landscape is provided by small basins containing seasonal lakes (called playas or salinas), dry valleys or draws, and dunes. Sediments in these features contain the archaeological sites that formed the basis of this study, and because one of our goals was to understand how or whether depositional context might effect the OSL results, we describe these settings briefly here.

The draws are (usually) dry tributaries of rivers to the east, and are incised into the Blackwater Draw Formation. Where incision intersected the groundwater table (the Ogallala Aquifer underlies this region), freshwater springs emerge, supporting a local flora and fauna, and attracting human foragers. Some of the richest archaeological sites in the region, including several in our sample, are in this setting. However, sites are found in other places along these draws. Sediments in this setting vary depending on local hydrology, but overall the stratigraphy is broadly similar throughout most of the draws, suggesting similar geomorphic responses to late Quaternary climatic and environmental change [19,20]. The most striking and often most stratigraphically visible of those changes is the period of Middle Holocene (Altithermal) aridity.

Playas are small, seasonally wet, internally drained lake basins inset into the Blackwater Draw Formation. Although these settings were undoubtedly attractive to prehistoric inhabitants, few have yielded in situ archaeological remains [21], though we suspect this is in large part an artifact of sampling and lack of exposures. The most common deposit is lacustrine mud, but slope wash and eolian deposits are found in larger basins [25].

Dunes are found either in large sand dune fields or as localized lunettes along the margins of playas. Several major west-to-east trending dune fields along the western escarpment of the Southern High Plains probably are derived from sands in the Pecos River valley that blew up into reentrant valleys onto the High Plains surface during the late Quaternary [24,34]. Archaeological remains are locally common, but often in settings of complex stratigraphic history. Lunettes are composed of silts, sands and carbonates deflated from the adjacent playas [22]. Few in situ archaeological sites within lunettes are known.

3. Archaeological framework

The archaeological components in our sample range from Late Glacial through Middle Holocene in age, though in several localities we also dated younger and non-archaeological strata as well. Several archaeological complexes are represented from this swath of time, including Early Paleoindian (marked by the stylistically distinctive Clovis and Folsom fluted points) and Late Paleoindian (marked by a variety of unfluted lanceolate forms). The Clovis and Folsom complexes are reasonably well dated by radiocarbon, and span the periods from 11,400 to 10,900 ^{14}C yr B.P., 10,900 to 10,200 ^{14}C yr B.P., respectively [14,15,23]. The Late Paleoindian period is not as well constrained chronologically, in part because of typological blurring and overlap in time and space [23,43]. In general, sites of this period range from 10,000 to 8000 ^{14}C yr B.P., but one of our goals was to gain better site-specific age control on some critical localities, including a couple of ‘‘type’’ sites.

We also include sites with later occupations, including Archaic sites (ca. 8000 to 6000 ^{14}C yr B.P.) which preserve rare traces of human occupation during the Altithermal of the Middle Holocene, when the region was subject to severe and prolonged drought [32]. Tying the Archaic record with the geologic record of desiccation should increase understanding of the nature of human adaptation, but almost no dates are presently available for the early and middle Archaic.

4. Samples

Samples are listed in Table 1 and site locations are shown in Fig. 1. Stratigraphic proveniences of individual samples are described below, using nomenclature from Holliday [21]. Simplified profile schematics are given in Fig. 2, but more detailed illustrations of stratigraphic contexts can be found in Holliday [21].

4.1. Samples from draws

Several samples were collected at Lubbock Lake (Texas), located on an entrenched meander of Yellowhouse Draw. More than 100 radiocarbon dates, obtained mostly from

Table 1
OSL sample locations

Lab #	Site	Stratum	Depositional context
UW479	Lubbock Lake	4A	Alluvial sand
UW480	Lubbock Lake	2m, top	Paludal mud/loam
UW568	Lubbock Lake	5A, Bw horizon	Slopewash/eolian sand
UW569	Lubbock Lake	4B, A horizon	Eolian sand
UW570	Lubbock Lake	4B, Btk-horizon	Eolian sand
UW571	Lubbock Lake	2s, top	Eolian sand
UW572	Lubbock Lake	3c	Marl
UW573	Lubbock Lake	IX, Late Holocene sand	Lunette
UW574	Lubbock Lake	VI, Early Holocene sand	Lunette
UW575	Ted Williamson	Upper Paleoindian sand	Dune sand
UW576	Ted Williamson	Lower Paleoindian sand	Dune sand
UW577	Milnesand	Paleoindian sand	Dune sand
UW578	Milnesand	20th Century fence dune	Eolian sand
UW579	San Jon	4s, base	Slopewash/eolian sand
UW580	San Jon	2s	Slopewash/eolian sand
UW582	Mustang Spring	4, top	Eolian sand
UW583	Mustang Spring	4, base	Eolian sand
UW584	Mustang Spring	3	Marl
UW585	Shifting Sands	VIII, Folsom sand	Dune sand
UW586	Bedford Ranch	VIII, Late Paleoindian sand	Dune sand
UW587	Bedford Ranch	IX, Late Holocene sand	Dune sand
UW588	Clovis	G1, Late Holocene sand	Dune sand

Strata designations are from Holliday [21].

organic rich lacustrine sediments or A-horizons but a few from charcoal [26,27], make it one of the better dated sites in the region. Folsom and Plainview cultural remains are found in stratum 2. Two samples from the top of this stratum were collected: UW480 from a paludal mud (2m) and UW571 from an eolian and slopewash derived sand lens on the valley margin (2s). UW572 was drawn from the overlying carbonate marl (3m). Other samples were taken from well-dated eolian or slopewash contexts higher in the stratigraphy: UW479 (4s), UW570 (4s), UW569 (4s, A-horizon), and UW568 (5s) (see Table 3.5 of Holliday [21]).

Three samples were collected from Mustang Springs (Texas), a Middle Holocene-age water ''wellfield'' dug into early Holocene lacustrine carbonate and diatomite [31,33]. UW584 was taken from the carbonate marl (Stratum 3), the deposit from the alkaline lake that likely represents the onset of warmer and drier Middle Holocene conditions, and which ultimately formed the surface from which the wells were dug. Two additional samples were collected from the base (UW583) and the top (UW582) of the aeolian deposit, a sandy loam (Stratum 4) that buried the wellfield [31]. Radiocarbon dates are available on both of these units at Mustang Springs.

Finally, a single sample, UW588, was taken from a well-dated Late Holocene stratum (G1, eolian sand) at Blackwater Locality No. 1 (New Mexico), the Clovis type site.

4.2. Samples from dunes

Two samples were collected from a well-dated lunette at Lubbock Lake. A consistent series of radiocarbon dates have been obtained from buried soils dividing the strata [17]. UW574 was collected from the mid-Holocene Stratum V and UW573 was collected from the late Holocene Stratum IX.

Several samples were collected from archaeological sites in two of the large dune belts that cross the western Llano Estacado. Three samples were collected from Andrews Dunes, one from Shifting Sands, and two from Bedford Ranch (Texas). The stratigraphy at these sites has been divided into ten units [21]. At Shifting Sands, Folsom/Midland artifacts have been recovered from Unit VIIb, a reddish brown loamy sand, and the bottom of Unit VIII, a thick, well-sorted eolian sand characterized by clay lamellae, probably illuvial in origin. UW585 from Shifting Sands was drawn from Unit VIII. No radiocarbon dates are available from this site. At Bedford Ranch, Firstview artifacts have been recovered from Unit VIII. UW586 was taken from that unit and UW587 was drawn from a radiocarbon-dated Late Holocene sand, Unit IX.

Four samples were collected from the Lea Yoakum Dunes, at the Milnesand and Ted Williamson sites (New Mexico), which are located only 550 m apart [7,21,42,49]. Exposed by blowouts, both sites contained an extensive *Bison antiquus* bonebed associated with Paleoindian artifacts, the type assemblage for the Milnesand site and a Plainview assemblage at Ted Williamson. There are no radiocarbon dates available for either of these sites. The bonebeds rest on the surface of the Blackwater Draw Formation but the bison skeletal remains and artifacts are also incorporated in the base of paleodune sands, which also contain clay lamellae. UW575 and UW576 were collected from upper and lower portions of the paleodune at Ted Williamson. At Milnesand the artifacts are incorporated in an A-horizon of the dune, from which UW577 was collected. UW578 was obtained from a modern sand accumulation behind a fence post, which based on information from local residents formed about 50 years ago. This sample will provide an opportunity to test the extent of bleaching in a modern setting.

4.3. Samples from playas

Two samples were collected from the San Jon site, in a large, heavily eroded playa on the northwest edge of the Southern High Plains. It contains a radiocarbon-dated stratified record of Paleoindian (the type site for San Jon points), Archaic and late Prehistoric occupations [16,41,50]. The archaeological materials are from the fill of a smaller basin, which is cut into fill of a larger basin. Toward the margins of the smaller basin, the fill consists of a series of four muds separated by sandy loams interpreted as slope wash. The Paleoindian artifacts are located in the second mud layer (2m) and UW580 was collected just above it in a sand layer (2s). UW579 was collected from the base of 4s, just above 4m.

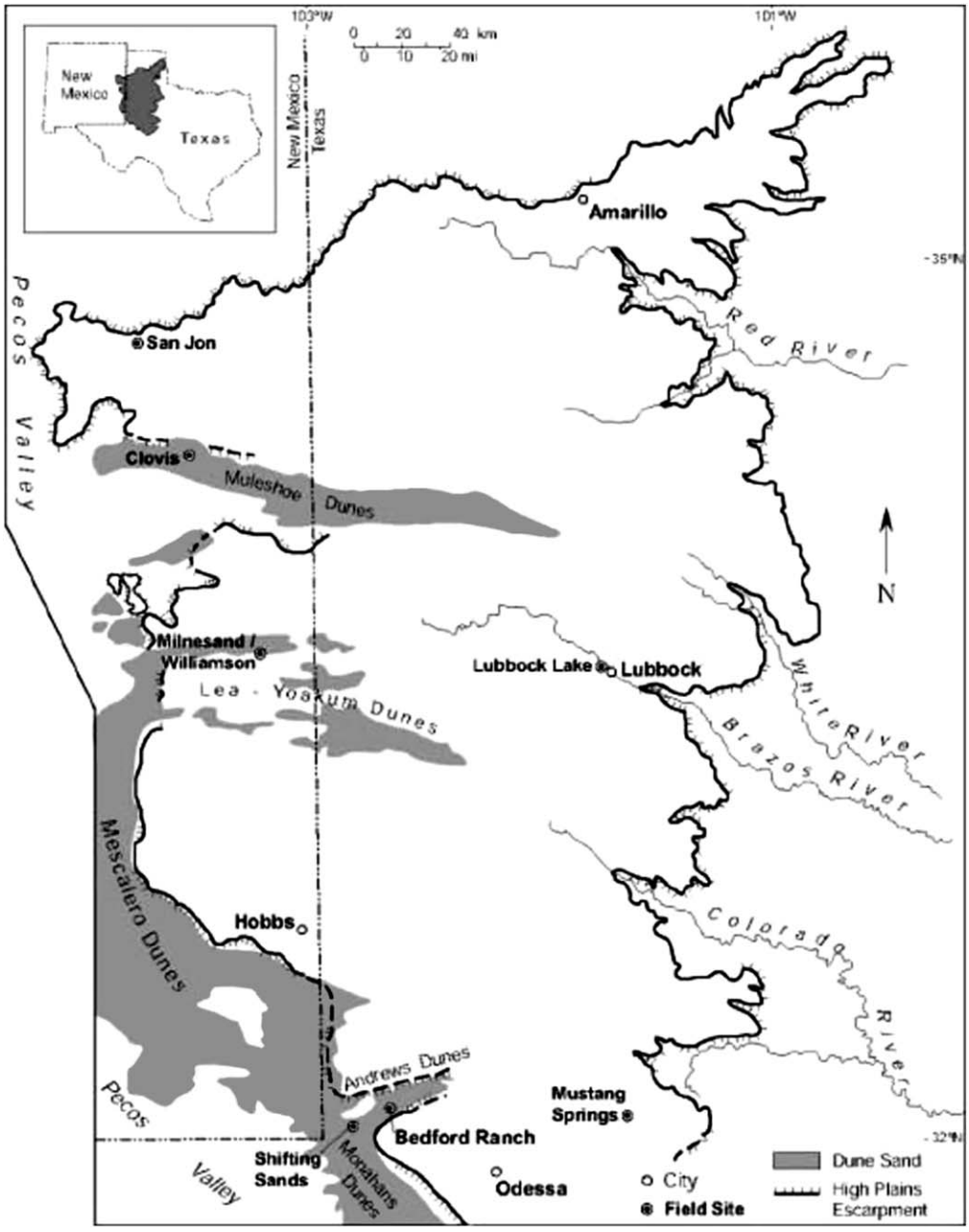

Fig. 1. Map showing location of sites discussed in the text.

5. Methods

A qualitative assessment of the luminescence results was reported earlier [10]. These results have now been modified by the collection of additional data and the application of more quantitative statistics.

Samples were collected by driving light-tight cylinders into exposed profiles, except for the three samples from Mustang Springs, which were collected without light exposure by a Giddings soil-coring rig. Radioactivity was measured in the laboratory by alpha counting, flame photometry and beta counting and in the field by in situ gamma spectrometry and by $CaSO_4$:Dy dosimeters.

Luminescence measurements were performed for most samples on 90–125 μm quartz, extracted using standard procedures [1]. Single-grain OSL was measured on a Risø TL-DA-15 apparatus with a single-grain attachment. The sample holders used for this equipment have holes to accommodate 180–212 μm grains. Visual inspection showed that on average three of the smaller sized grains fit into these holes, compromising single-grain resolution. However, many grains in these samples have no measurable luminescence signal. At best only a quarter of the positions produced a signal, meaning that the chance of two luminescence-producing grains occupying the same hole is less than 18%. But the percentage of positions producing a signal is greater than the

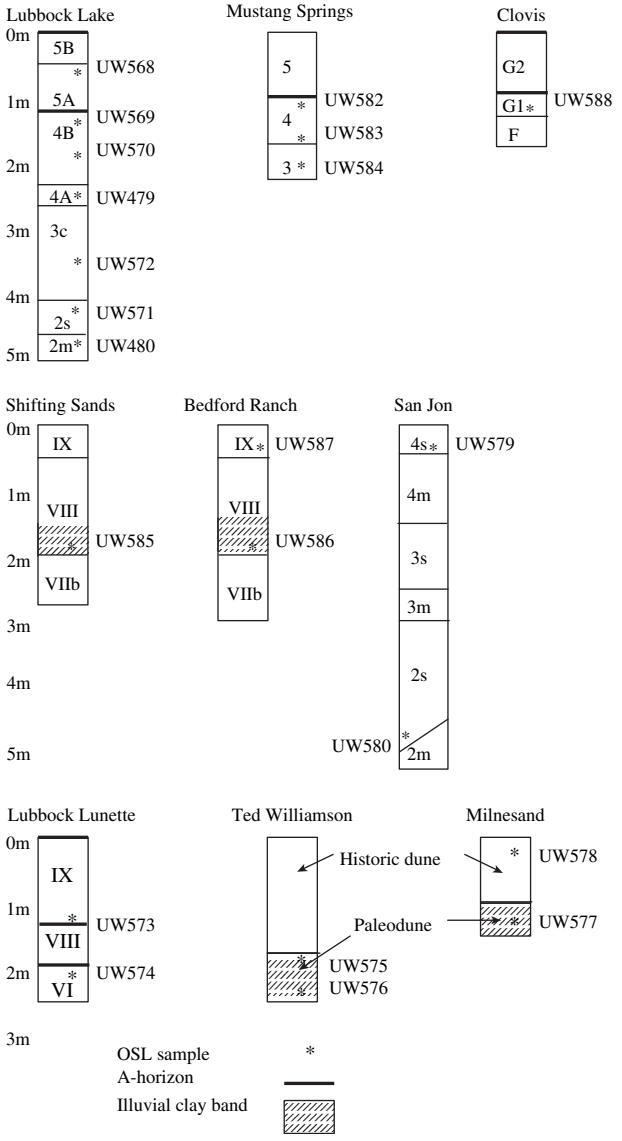

Fig. 2. Vertical stratigraphic relationships of samples. Samples were not necessarily collected in a single vertical column, but horizontal relationships are omitted for ease of illustration. Locations of a-horizons and illuvial clay bands are also shown. Sources of data: Lubbock Lake [20], Mustang Springs [31], Clovis [24], Shifting Sands, Bedford Ranch, Ted Williamson, and Milnesand [21,24], Lubbock lunette [22].

percentage of grains with signals. If only 15% of *grains* produce a signal, the probability of two luminescence-producing grains occupying the same position is 7%. This provides near single-grain resolution, while at the same time increasing the chances that the position will produce a measurable signal.

Equivalent dose (D_e) was determined by the single aliquot regenerative dose (SAR) method [36], with parameters given in Table 2. Equivalent dose was also determined on multi-grain aliquots, containing ~1000 grains each, but these results are not discussed as they are fully consistent with, but have less resolution than, the single-grain results. On two samples, UW572 and UW584, which contained few coarse grains, fine-grain analysis using a multi-aliquot IRSL procedure was employed.

Table 2
Single-grain OSL measurement parameters

System	Risø TL-DA-15, single-grain attachment
Excitation	532 nm laser (90% power)
Detection filters	7.5 mm U340 (ultraviolet)
Preheat	240 °C 10 s
Cut heat	160 °C
Test dose	2–5 Gy
Exposure	0.8 s at 125 °C
Analysis	0.06 s, background 0.65–0.8 s
SAR sequence	Dose (D_i, where $i = 0$ for natural signal) Preheat OSL (L_i) Test dose Cut heat OSL (T_i) Repeat steps for i = different regeneration doses, including a zero dose and a repeat dose

6. Single-grain OSL dating

Single-grain dating became feasible in recent years through developments in both method [36] and instrumentation [5]. The rationale for dating single grains arises from the possibility that either all grains were not fully reset by daylight (“bleached”) at time of deposition or grains of different ages were mixed after. If either is true, then a multi-grain luminescence analysis will produce an average D_e that may have little meaning. The distribution of D_e values from single grains, on the other hand, may allow detection of differential bleaching or mixing.

Yet, dating single grains is not without complications. Even if all grains were fully bleached at deposition, D_e will vary from grain to grain for a number of reasons that include differential precision, variation in radiation dose rates, variation in other luminescence properties, and non-uniformity in artificial dose applications [13,47]. These effects are random, however, and a working assumption is that a narrow, normally distributed distribution of D_e values represents a well-bleached, unmixed assemblage of grains [48]. How narrow does it have to be and is normality either a sufficient or necessary criterion? Galbraith et al. [12,13] have defined an over-dispersion value (σ_b) to represent variation that cannot be accounted for by the differential precision arising from counting statistics. Empirical evidence has suggested that well-bleached, unmixed single-grain distributions have an over-dispersion value less than about 20% [38].

Interpretation of skewed distributions has followed theoretical expectations of particular geological processes, such as fluvial deposition [28,37] or mixing and disturbance in soils [8], which can lead to partial bleaching. Under such circumstances, only grains with smaller D_e values, minimum age estimations, reliably inform on the age of the deposit. Minimum ages might also be appropriate in cases where other geological and geomorphic processes are active [38]. What portion of the distribution represents the true age is much less clear in circumstances of post-depositional mixing or disturbance, where multi-modality might be present [4].

Galbraith et al. [12] introduced statistical models that we apply to single-grain D_e distributions in this work. The *central age model* is similar to a weighted mean, except that a natural normal distribution rather than a single true value, making it more appropriate for single grains, is assumed. Log values of D_e are also used to avoid various statistical problems [13]. If a single true value is assumed, the statistic is called the *common age model*. The *minimum age model* in effect segregates those grains at the low end of the distribution that could form a single-aged population. In this work, the central and common age were calculated by a program written by Hiro Yoshida (University of Wollongong, Australia) and the minimum age by an optimization program written by Geoff Laslet (CSIRO Mathematical and Informational Services, Melbourne). The central age program also calculates overdispersion (σ_b).

7. Results

7.1. Dose rate

Radioactivity data presented in Tables 3 and 4 reflect an overall consistency among the different laboratory and field measurements employed (see Figs. 1 and 2 in Feathers [10]). Two possible sources of dose rate change through time should be considered. One is clay illuviation, which is apparent in the large dunes. Clay enriched in radioactive sources could increase radioactivity of the paleo-dunes through time. The other is leaching of carbonates, which likely took place over time in the Lubbock Lake lunette. The sediments today have 15–18% carbonate, but were deflated from marls, which were probably much higher in carbonate [17,22]. Current carbonate levels also represent secondary leaching from younger sediments.

7.2. Fine-grained samples

For UW572 (Lubbock Lake) and UW584 (Mustang Springs), both fine-grained marls, 4–11 μm grains were isolated by settling in acetone. D_e was measured by multi-aliquot infrared stimulated luminescence (IRSL) using the slide method [39]. Irradiated aliquots were stored for 1 week prior to measurement. A fading test, where equally dosed aliquots were stored for different times up to 8 weeks, showed little fading for either sample after one day storage. The D_e derived is 13.8 ± 1.4 Gy for UW572 and 16.3 ± 1.3 Gy for UW584, both using linear fits to the growth curves.

7.3. Dose recovery

To make sure that SAR procedures to determine D_e can potentially yield the correct answer, a dose recovery test was employed by exposing sample aliquots to enough light to reduce the luminescence signal to background, then administering a known dose, and finally making an estimate of this dose using SAR. A 17.5 Gy dose was applied to 400 grains from each of five samples. Table 5 shows resulting D_e using the common age model and also the number of grains within one and two standard errors of the administered dose. The

Table 3
Radioactivity

Sample	^{238}U (ppm)	^{232}Th (ppm)	K (%)	Beta dose rate (Gy/ka)	
				β-counting	α-counting/flame photometry
UW479	2.18 ± 0.16	6.16 ± 1.00	0.61 ± 0.01	0.763 ± 0.053	0.960 ± 0.037
UW480	2.41 ± 0.19	8.44 ± 1.19	1.00 ± 0.02	1.249 ± 0.082	1.361 ± 0.045
UW568	1.86 ± 0.15	6.64 ± 1.04	0.92 ± 0.01	1.104 ± 0.080	1.173 ± 0.036
UW569	2.42 ± 0.20	10.09 ± 1.34	1.52 ± 0.04	1.753 ± 0.121	1.816 ± 0.055
UW570	2.92 ± 0.22	10.33 ± 1.34	1.43 ± 0.02	1.690 ± 0.117	1.825 ± 0.050
UW571	2.79 ± 0.20	7.27 ± 1.12	0.71 ± 0.02	1.129 ± 0.08	1.164 ± 0.044
UW572	4.25 ± 0.23	1.29 ± 0.58	0.37 ± 0.01	0.943 ± 0.062	0.955 ± 0.038
UW573	2.21 ± 0.18	7.37 ± 1.10	0.78 ± 0.03	0.997 ± 0.065	1.134 ± 0.047
UW574	3.19 ± 0.20	4.85 ± 0.92	0.74 ± 0.02	1.148 ± 0.081	1.176 ± 0.041
UW575	0.41 ± 0.05	2.73 ± 0.48	0.44 ± 0.01	0.687 ± 0.046	0.478 ± 0.016
UW576	0.77 ± 0.07	1.69 ± 0.50	0.38 ± 0.02	0.498 ± 0.034	0.457 ± 0.021
UW577	0.72 ± 0.07	2.35 ± 0.59	0.42 ± 0.02	0.564 ± 0.045	0.500 ± 0.023
UW578	0.41 ± 0.06	1.99 ± 0.53	0.48 ± 0.03	0.590 ± 0.039	0.491 ± 0.031
UW579	0.71 ± 0.20	19.65 ± 1.90	1.52 ± 0.01	1.757 ± 0.114	1.828 ± 0.060
UW580	1.90 ± 0.21	14.96 ± 1.64	1.35 ± 0.03	1.775 ± 0.116	1.744 ± 0.060
UW581	1.66 ± 0.14	7.10 ± 1.00	1.24 ± 0.03	1.457 ± 0.112	1.403 ± 0.043
UW582	3.18 ± 0.22	7.57 ± 1.13	1.15 ± 0.08	1.501 ± 0.098	1.607 ± 0.059
UW583	3.45 ± 0.22	7.07 ± 1.02	1.18 ± 0.01	1.618 ± 0.105	1.628 ± 0.043
UW584	3.48 ± 0.27	4.52 ± 0.73	0.36 ± 0.01	1.044 ± 0.069	0.911 ± 0.046
UW585	0.43 ± 0.05	2.30 ± 0.42	0.18 ± 0.01	0.287 ± 0.027	0.268 ± 0.15
UW586	0.48 ± 0.04	0.98 ± 0.27	0.14 ± 0.01	0.243 ± 0.027	0.232 ± 0.15
UW587	0.26 ± 0.05	1.50 ± 0.35	0.10 ± 0.01	0.208 ± 0.021	0.174 ± 0.017
UW588	0.71 ± 0.06	1.94 ± 0.41	0.57 ± 0.03	0.637 ± 0.044	0.604 ± 0.030

U and Th values given in ppm of the parent. Beta dose rate was calculated in two different ways: directly from beta counting and indirectly from alpha counting (assuming secular equilibrium) plus flame photometry for K.

Table 4
External dose rate determined in three ways

Sample	External dose rate (Gy/ka)		
	In situ gamma spectrometry	In situ dosimetry	Laboratory
UW479	0.751 ± 0.033	0.975 ± 0.155	0.811 ± 0.065
UW480		1.419 ± 0.146	0.914 ± 0.070
UW568	0.944 ± 0.041	0.908 ± 0.214	0.929 ± 0.078
UW569	1.040 ± 0.042	1.131 ± 0.101	1.238 ± 0.090
UW570		1.574 ± 0.057	1.317 ± 0.086
UW571	0.950 ± 0.043	1.132 ± 0.293	0.888 ± 0.070
UW573	0.847 ± 0.040		0.974 ± 0.087
UW574	0.893 ± 0.040		0.876 ± 0.073
UW575-6	0.559 ± 0.034	0.686 ± 0.058	0.463 ± 0.050
UW577	0.725 ± 0.036		0.497 ± 0.053
UW578		0.540 ± 0.046	0.530 ± 0.076
UW579	1.357 ± 0.061	1.737 ± 0.325	1.560 ± 0.106
UW580	1.339 ± 0.061	1.663 ± 0.062	1.378 ± 0.107
UW581	0.910 ± 0.036	1.186 ± 0.146	0.982 ± 0.079

Laboratory measurements are derived from alpha counting (assuming secular equilibrium) and flame photometry.

common age D_e is within error terms of 17.5 Gy for all samples. The percentage of grains within 1- and 2-sigma is better than or close to the expected values of 67% and 95%. We conclude that SAR is working for these samples.

7.4. Feldspar contamination

A test for feldspar contaminates in the quartz samples compared sensitivity corrected responses on multi-grain aliquots to two identical doses, one of which was followed by an IRSL exposure. A ratio of these responses greater than the average recycling ratio suggested the presence of some feldspars on three samples UW576, UW580 and UW582 (from Ted Williamson, San Jon, Mustang Springs, respectively). For these three samples, 300 individual grains were measured using SAR but including two doses followed by an IRSL exposure prior to the OSL measurement. Of the 83 measurable grains, none could be identified as feldspar. In another test, 100 randomly selected grains from UW479 (Lubbock Lake) were analyzed individually by an X-ray attachment to a scanning electron microscope. Silicon was the only element detected for all of them, giving no evidence of feldspar contamination. While some feldspar contamination is present in some of these samples, we conclude the effect is slight.

Table 5
Dose recovery results

Sample	No. of accepted grains	Equivalent dose (Gy) (common age model)	% of grains within 1σ of 17.5 Gy	% of grains within 2σ of 17.5 Gy
UW479	77	18.0 ± 0.5	81.8	96.1
UW480	88	18.0 ± 0.5	84.1	94.3
UW576	34	18.3 ± 0.9	88.2	97.1
UW580	22	18.2 ± 0.8	90.1	95.5
UW583	56	17.1 ± 0.6	87.5	96.4

7.5. Single-grain analysis

At least 900 grains were measured for each sample. Grains were rejected from analysis if (1) the error on the test dose exceeded 20% or the net natural signal was less than three times the standard deviation of the background, (2) the ratio of L_i/T_i for repeated regeneration doses was outside 0.8–1.2, (3) the natural signal was significantly higher than the signal from the highest regeneration point, (4) the signal from a zero dose was greater than 10% of the natural signal, and (5) the error on D_e was greater than 100%. Few grains were eliminated for any sample for any of the last three criteria. The last criterion was not applied in the case of the only modern sample, UW578 (Milnesand). Table 6 gives the ratio of accepted to measured grains. The wide variation in acceptance ratio is a function of defect composition and diverse histories of bleaching and irradiation. An attempt was made to secure at least 100 acceptable grains for each sample, but for some samples this was not time-effective.

The distribution of D_e values among individual grains are displayed as radial graphs [12] and weighted histograms, selected examples shown in Fig. 3. The radial graphs allow visualization of over-dispersion, represented by those points beyond two standard errors of a reference. The weighted histograms show the distribution shape.

On suspicion that σ_b might depend on sample size, Fig. 4 was drafted to show that smaller sample sizes do indeed have high over-dispersion values. But so do some of the larger sample sizes. If those points represented by diamonds are removed, the remaining points roughly fit to an exponential regression line ($r^2 = 0.5$). Above about 75 grains, over-dispersion values level off at about 20%, close to the cut-off value Olley et al. [38] observed for single-aged samples. We assume that

Table 6
Number of grains (positions) measured and accepted for each sample

Sample	Total grains	Accepted	Acceptance ratio
UW479	1000	226	0.226
UW480	1000	172	0.172
UW568	1000	182	0.182
UW569	1000	101	0.101
UW570	999	141	0.141
UW571	900	145	0.161
UW573	999	125	0.125
UW574	999	197	0.197
UW575	1500	73	0.049
UW576	1497	107	0.071
UW577	2392	116	0.049
UW578	995	70	0.074
UW579	999	17	0.017
UW580	1997	115	0.058
UW582	1400	83	0.059
UW583	1000	142	0.142
UW584	130	25	0.192
UW585	2495	47	0.019
UW586	2598	51	0.020
UW587	2298	44	0.019
UW588	1000	19	0.019

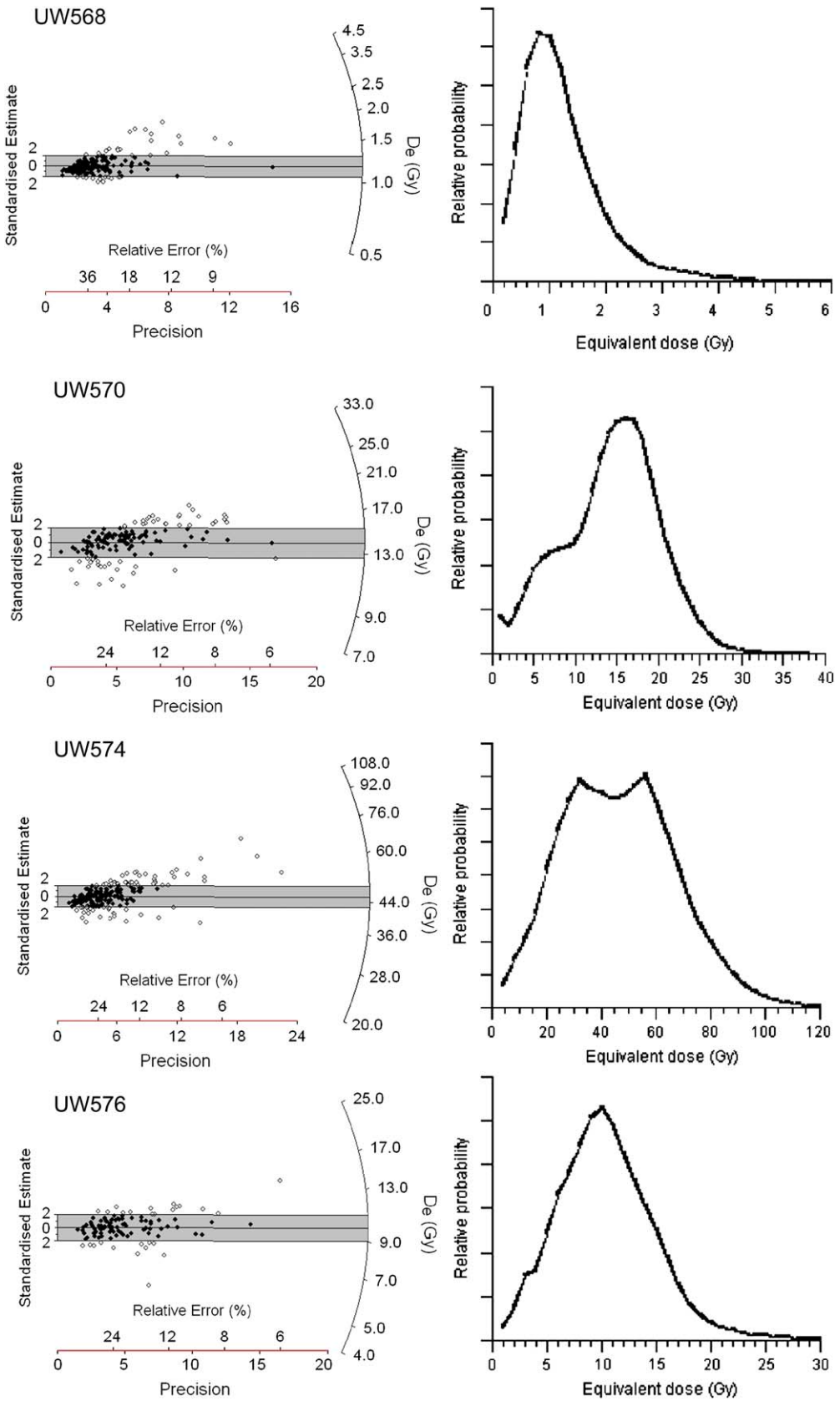

Fig. 3. (Left) Radial graphs of selected samples. The first six samples have relatively high over-dispersion values, the last four relative low over-dispersion values. Radial graphs plot precision (reciprocal of relative error) against a standardized value for D_e. Values are standardized as the number of standard errors away from some reference point, in most cases the D_e determined by the central age model. The shaded area includes all points within two standard errors of the reference. A line drawn from the origin through any point will intersect the right axis at the true D_e. Two references are drawn for UW577, one the minimum age model and one the central age model after the minimum points have been removed (see text). The reference point for UW583 is the trailing edge. The radial graphs were constructed using a program written by Jon Olley. (Right) Weighted histograms of the same samples, constructed by summing normal probability density plots for each value.

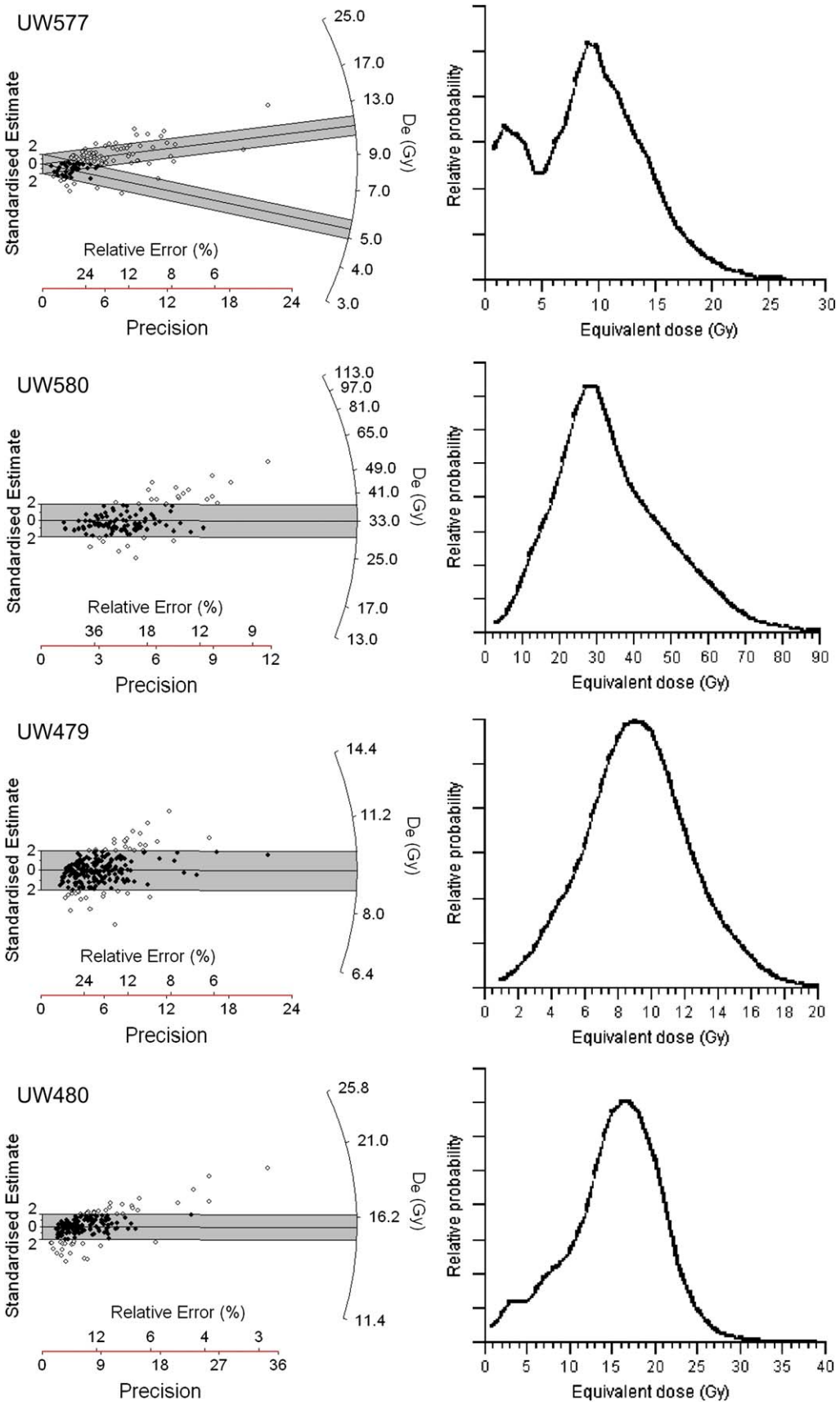

Fig. 3 (*continued*).

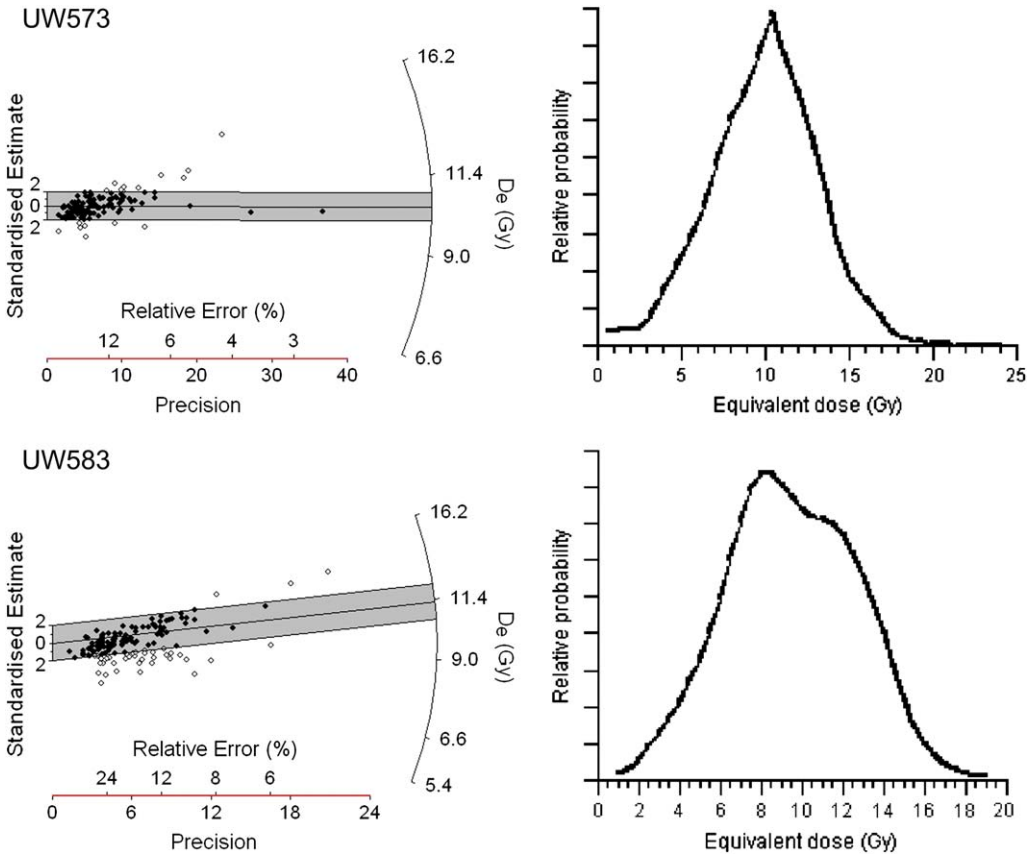

Fig. 3 (*continued*).

these samples are composed of single-aged grains, while those above the exponential fit (diamonds) consist of multiple-age grains, either because of partial bleaching or post-depositional mixing. For those with small sample size, whether the grains are single-aged or not cannot be reliably determined.

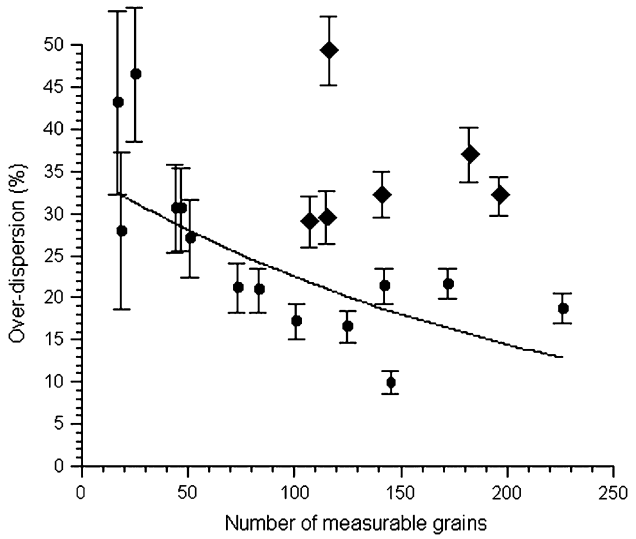

Fig. 4. Over-dispersion as a function of sample size. The line represents an exponential fit to the data points represented by circles. Points significantly above this line, shown as diamonds, are considered to have over-dispersion values inconsistent with a single-aged sample.

Table 7 gives the central age and minimum age D_e values and the over-dispersion values (σ_b). The minimum age model requires an estimation of over-dispersion expected of well-bleached samples. We averaged the over-dispersion of the seven samples considered well bleached and with sufficient sample size in Fig. 4. This came to 18% and was added in quadrature to all equivalent dose estimations prior to determining the minimum age [13].

The D_e distributions of the six samples with high over-dispersion (and relatively large sample size) are displayed in Fig. 3, along with four examples of low over-dispersion samples. To test whether the over-dispersion is caused by partial bleaching or post-depositional mixing, $D_e(t)$ plots and linear-modulated (LM) OSL curves [44] were generated for the over-dispersed samples and two of the low-dispersion samples. Both procedures take advantage of the fact the quartz OSL signal is composed of different components that bleach at different rates [3]. $D_e(t)$ plots compare D_e values determined at different intervals of the OSL decay curve, on the justification that earlier intervals are dominated by faster bleaching components and later intervals by slower bleaching components. Higher D_e values for later intervals indicate partial bleaching. Because the laser in single-grain analysis reduces the OSL signal quite rapidly, only three intervals were chosen for analysis: 0–0.03 s, 0.03–0.08 s and 0.08–0.16 s. Even

Table 7
Equivalent dose determinations

Sample	*N*	Equivalent dose (Gy)		% Over-dispersion (σ_b)
		Central age model	Minimum age model	
UW479	226	9.33 ± 0.17	8.97 ± 0.57	18.7 ± 1.7
UW480	172	15.67 ± 0.33	14.83 ± 1.05	21.6 ± 1.8
UW568	182	1.17 ± 0.04	0.79 ± 0.04	36.9 ± 3.3
UW569	101	6.49 ± 0.15	6.48 ± 0.38	17.2 ± 2.1
UW570	141	14.00 ± 0.45	11.36 ± 0.80	32.2 ± 2.6
UW571	145	14.52 ± 0.20	14.16 ± 0.45	9.9 ± 1.4
UW573	125	10.37 ± 0.22	10.24 ± 0.52	16.5 ± 1.9
UW574	197	45.70 ± 1.27	34.03 ± 0.21	32.1 ± 2.3
UW575	73	9.73 ± 0.32	9.11 ± 0.91	21.1 ± 3.0
UW576	107	10.04 ± 0.36	8.12 ± 0.66	29.0 ± 3.0
UW577	116	8.43 ± 0.44	5.27 ± 0.67	49.2 ± 4.1
UW578	70	0.12 ± 0.02	NA	NA
UW579	17	2.86 ± 0.37	1.80 ± 0.52	43.1 ± 10.9
UW580	115	33.38 ± 1.18	25.94 ± 2.74	29.5 ± 3.1
UW582	83	7.67 ± 0.23	7.03 ± 0.70	20.9 ± 2.6
UW583	142	9.63 ± 0.23	8.67 ± 0.70	21.3 ± 2.1
UW584	25	13.17 ± 1.35	8.08 ± 1.68	46.5 ± 8.0
UW585	47	7.34 ± 0.41	5.70 ± 0.78	30.5 ± 4.9
UW586	51	4.10 ± 0.21	3.41 ± 0.51	27.0 ± 4.6
UW587	44	3.46 ± 0.21	2.75 ± 0.40	30.5 ± 5.2
UW588	19	1.07 ± 0.10	0.84 ± 0.19	27.9 ± 9.3

Central age model could not be calculated for UW578; value is from common age model [12].

then only the first or first two intervals produced measurable results on many grains. LM-OSL allows faster and slower components to be more easily resolved, but for single grains requires considerable machine time. Only limited data were collected, ramping the laser from 0 to 90% power over 20 s, using the first 1 s to represent the fast component and the last 1 s as a slower component. The first 0.2 s, when the laser was less than the 5% power used to orient disks, was used as background. On most measurable grains, either the fast component or the slower component could be measured, but rarely both.

Table 8 shows the $D_e(t)$ results. The central age D_e was computed from measurable grains for each interval and also for the first interval only from those grains that had measurable signals at all three intervals. The second part of the table tabulates the number of grains where the first interval was equivalent to or less than the last interval. On only three samples (UW480, UW577, and UW580 [Lubbock Lake, Milnesand, and San Jon]), each from very different stratigraphic contexts, was the D_e from the last interval significantly higher at 1-sigma than that from the first interval. None were significant at 2-sigma. On only one samples, (UW570 [Lubbock Lake]) was the later interval significantly higher than the earlier interval when comparing only those grains where all three intervals could be measured. This is the only sample that also had a high proportion of individual grains where the last interval was higher than the first interval. The LM-OSL results were less meaningful. Only 98 grains (of about 2000) from seven samples produced a measurable signal. On four samples no slow component was measurable, and on two others only 5 grains total had a slow component. Only UW574 (Lubbock Lake lunette) produced even minimal numbers (19 fast components, 10 slow components, four grains with both) and on this sample the central age D_e from the two components did not differ, and on only one of the four grains did the slow component exceed the fast.

Without doubt some grains in these samples were not well bleached at the time of deposition. However, the effect appears

Table 8
$D_e(t)$ data for eight samples

Sample	0–0.03 s		0.03–0.08 s		0.08–0.16 s		0–0.03 s	
	N	D_e (Gy)	*N*	D_e (Gy)	*N*	D_e (Gy)	*N*	D_e (Gy)
UW480	182	16.2 ± 0.4	59	17.1 ± 0.6	21	18.1 ± 1.0	21	15.9 ± 1.2
UW568	184	1.19 ± 0.05	56	1.15 ± 0.09	23	1.37 ± 0.14	23	1.32 ± 0.16
UW570	149	14.5 ± 0.5	39	14.2 ± 0.8	14	15.8 ± 0.9	14	9.11 ± 1.37
UW574	203	47.4 ± 1.3	70	48.4 ± 2.1	22	51.5 ± 3.4	22	47.7 ± 3.7
UW576	95	10.0 ± 0.4	30	10.0 ± 0.7	10	9.82 ± 1.05	10	10.7 ± 1.0
UW577	108	8.79 ± 0.52	38	10.0 ± 0.8	15	11.2 ± 1.2	15	10.8 ± 1.3
UW580	117	35.0 ± 1.4	40	35.0 ± 1.8	19	39.4 ± 2.9	19	37.0 ± 2.5
UW583	149	9.73 ± 0.28	53	9.07 ± 0.58	17	8.04 ± 1.00	17	10.2 ± 0.7

Sample	N	1st interval ≥ 3rd interval	1st interval < 3rd interval
UW480	21	18	3
UW568	23	23	0
UW570	14	7	7
UW574	22	18	4
UW576	10	10	0
UW577	15	14	1
UW580	19	17	2
UW583	17	15	2

Values in the top table give the D_e (central age model) for three time intervals of the decay curve. The last column repeats the first interval data except that it includes only those grains where the third interval could also be measured. Values in the bottom table are the number of grains where the D_e of the first interval is more or less than that of the third interval, counting only grains where both could be measured.

to be minimal (compare the very slightly rising $D_e(t)$ plots for UW480, UW577 and UW580 [Lubbock Lake, Milnesand, and San Jon] with the poorly bleached fluvial sediments illustrated in Singarayer et al. [44]). This is perhaps not surprising given the large aeolian component in most samples, but it was also true for UW480, which is from a paludal mud with some aeolian sediments added.

High over-dispersion of some samples is therefore more likely explained by post-depositional mixing. The shapes of the weighted histograms (Fig. 3) also are not typical of poorly bleached samples [28]. An exception is UW568 (Lubbock Lake), but the skewness of this sample probably reflects its near surface location. In other samples, distributions exhibit modality that is more likely caused by turbation. Modality is particularly marked in UW577 (Milnesand) and UW574 (Lubbock Lake lunette), somewhat less so in UW570 (Lubbock Lake) and even appears as a pronounced shoulder in a low-over-dispersion sample such as UW583 (Mustang Springs).

Further evidence for well bleaching comes from UW578, a sample collected from sand build-up behind a historic fence post at Milnesand. The D_e values are consistent with a single age (no over-dispersion could be calculated) and the age, using the common age model, of AD 1880 ± 20 is somewhat older than the local residents suggest but still indicating a fairly well-bleached sample.

With little evidence for partial bleaching, the minimum age model is not necessarily a good choice for the depositional age of the high over-dispersion samples. But the central age model, best for the low over-dispersion samples, may not be justified either unless disturbance factors have moved as many grains up as down. In some cases, selecting the D_e from one of the modes or even using a ''trailing edge'' model has better justification. The derived ages and (where available) comparable independent radiocarbon ages are given in Table 9. The basis for the OSL age determinations is discussed in the next section.

8. Age determinations

OSL and independent ages are given in Table 9. Independent dating evidence, from both radiocarbon and multi-grain OSL [40], is especially strong in the case of Lubbock Lake. Other samples are from sites that have fewer available radiocarbon dates, or none at all. Estimates of the age of latter are routinely based on the occurrence of stylistically-distinctive projectile points, but these are, at best, ''ballpark'' estimates, and certainly cannot be used as independent cross-checks on the OSL results. The discussion that follows is arranged by geomorphic setting, beginning with the Lubbock Lake samples.

8.1. Samples from draws

Ages derived from the central age model at Lubbock Lake follow the correct stratigraphic order and reasonably agree with the radiocarbon dates (Fig. 5). The OSL ages differ significantly from the radiocarbon ages on only two samples, and the D_e distribution for both show some modality, suggesting admixture of younger grains. This effect is slight for UW570, which also has higher than normal over-dispersion, but more significant for UW480. Neither central age nor minimal age models may be appropriate for these two samples.

Table 9
Derived OSL ages

Sample	Site	Basis for age	Age (yr)	Independent ^{14}C age determination (yr)[a]
UW479	Lubbock Lake	Central age model	5640 ± 340	5800
UW480	Lubbock Lake	Central age model	7820 ± 460	9400
UW568	Lubbock Lake	Central age model	610 ± 40	500
UW569	Lubbock Lake	Central age model	2370 ± 130	2000
UW570	Lubbock Lake	Central age model	4850 ± 260	5600
UW571	Lubbock Lake	Central age model	7920 ± 450	8600
UW572	Lubbock Lake	Multi-aliquot fines	7770 ± 990	7000
UW573	Lubbock Lake	Central age model	5350 ± 350	1300
UW574	Lubbock Lake	Central age model	25300 ± 1600	7000–10000
UW575	Ted Williamson	Central age model	10400 ± 800	None
UW576	Ted Williamson	Central age model	11300 ± 900	None
UW577	Milnesand	High mode	11400 ± 800	None
UW578	Milnesand	Common age model	120 ± 20	None
UW579	San Jon	Central age model	900 ± 130	<1700
UW580	San Jon	Central age model	11800 ± 800	<9300–13500
UW582	Mustang Spring	Central age model	3840 ± 300	>2000
UW583	Mustang Spring	Trailing edge	6360 ± 600	7700
UW584	Mustang Spring	Central age model	9050 ± 1440	9000
		Multi-aliquot fines	9690 ± 1170	
UW585	Shifting Sands	Central age model	10600 ± 1200	None
UW586	Bedford Ranch	Central age model	7250 ± 830	None
UW587	Bedford Ranch	Central age model	7460 ± 880	2000
UW588	Clovis	Central age model	1030 ± 110	<1500

[a] All values are rounded approximations, not averages, and set to calendrical scale.

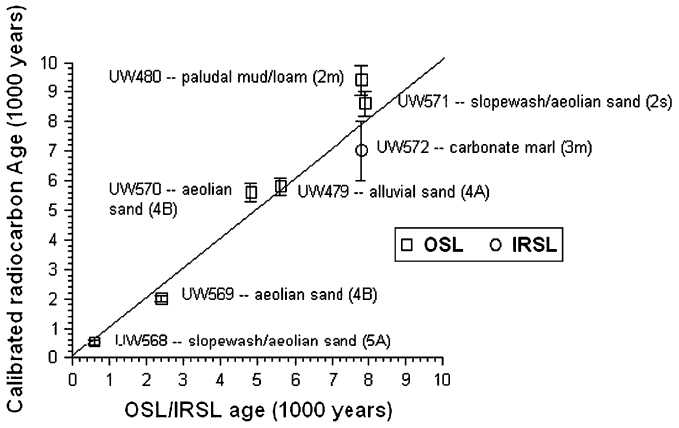

Fig. 5. Comparison of ages for Lubbock Lake samples using radiocarbon and luminescence.

The only other sample with high over-dispersion is UW568, but this may reflect closeness to the modern surface.

At Mustang Springs, UW584, from calcareous marl likely marking the onset of Altithermal conditions, contained little coarse-grained material, but enough for 25 single-grain analyses. The OSL age from these grains agrees well with the fine-grain results and both agree with the corresponding radiocarbon date. The other two Mustang Springs samples are from the top (UW582) and bottom (UW583) of an aeolian sandy loam burying the well field. Both samples have relatively low over-dispersion, suggesting minimal mixing, although the UW583 distribution has a pronounced shoulder on the upper side. For UW582 the central age model produces an age stratigraphically consistent with a radiocarbon age of about 2 ka from the next highest stratum. The central age from UW583 (4700 ± 300 yr) is much younger than expected given the corresponding radiocarbon ages. This sample is from just above a distinct boundary with the marl and probably not much mixing has occurred across the boundary. But slight mixing from above, such that the shoulder represents the oldest grains of the unit, is possible, making a ''trailing edge'' model appropriate. This was determined by subtracting all the D_e values from a large number and then calculating the minimum age from this reversed order. This produced an age of 6360 ± 600 yr, much more consistent with the radiocarbon results [31].

One final sample from a draw context is UW588 from Blackwater Locality No. 1. Although the sample size was small for this sample, the central age model produced an age, 1030 ± 100 yr, in agreement with radiocarbon determinations.

8.2. Samples from dunes

The derived ages from the Lubbock Lake lunette are badly overestimated in relation to the radiocarbon dates, which are believed to be correct based on associated faunal evidence. D_e distribution for UW574 is characterized by high over-dispersion and substantial modality, but little evidence of partial bleaching, while UW573 had one of the lowest over-dispersion values in the study. One cannot therefore justify for either sample a minimum age model, which still overestimates the ages at any rate. We suspect the discrepancy stems from underestimation of dose rate. The samples are high in carbonates and leaching or secondary precipitation may have reduced the dose rate through time.

The remainder of the samples from dunes are from deposits which lack independent age control. If, however, we use the ''ballpark'' estimates based on the projectile points found at these localities, we can at least determine whether the OSL ages are comparable.

The samples from the Lea Yochum dune field sites, Milnesand and Ted Williamson, yield intuitively satisfying post-Folsom OSL ages. Certainly, the OSL ages for Ted Williamson are in broad agreement with ages that might be expected, based on their associated projectile points (Plainview points), as these have been radiocarbon dated at other sites on the Plains.

Although we suspect that the Milnesand site and its projectile points are approximately the same age as those at Ted Williamson—and the OSL result certainly bears this out—there are no radiocarbon cross checks. Thus, this OSL result becomes the first chronometric date for these points. As such, a few comments in regard to its reliability are in order. The over-dispersion (49.2%) for the Milnesand sample, UW577, is the highest of any sample in this study and the D_e distribution is strongly bi-modal (Fig. 3). The minimum age model, which roughly characterizes the lower mode, produces an unreasonable age of about 5000 yr. The central age model also produces an age that seems too young. Removing all values less than 1-sigma above the minimum age model estimate and taking the central age of the remaining values yielded the D_e used to calculate the age. This is shown to well capture most of the high values (Fig. 3). The source of this bi-modality is unknown, but perhaps the sample collection tube partially intersected an animal burrow.

The quartz in the samples from the Andrews Dune Field is insensitive, so small sample size makes the results problematic. UW585 (Shifting Sands) is from a Folsom/Midland site. Although no Folsom/Midland site on the Southern High Plains has been successfully radiocarbon dated, if we use the approximate age of Folsom, the OSL central age is an underestimate by a couple of thousand years.

Sample UW586 (Bedford Ranch) yielded a central age of 7250 yr. The site has yielded Firstview points, and though the age of this particular style is not well constrained, we note that the OSL result is far younger in comparison [21,23]. More troublesome, the ages of UW586 and UW587 ought to be significantly different, as the latter was obtained from a Late Holocene deposit at the same site. Yet, the two OSL ages are identical, and UW587 appears much older than it ought to be. This discrepancy could suggest substantial mixing, but clay lamellae present in the paleodune suggest stability, and the modest over-dispersion values (considering sample size) do not suggest a multi-age sample.

Clay illuviation, possibly making the current radioactivity higher than it was in the past, could explain the age

underestimation for both UW585 and UW586, although this was not true in the Lea Yochum dune field samples where clay lamellae are also present. Another possibility is that the artifacts at Bedford Ranch and Shifting Sands were recovered from deflated surfaces and not the same age as the sands that contain them. Neither explanation can account for the extreme overestimation of UW587, which remains an anomaly.

Overall, the dune samples are the most troublesome in this study, but the reasons may relate to dose rate or association problems rather than dune deposition. (One should not therefore conclude from this that OSL dating of dunes will always be problematic. Many successes have been reported, e.g., [35].) Multi-grain analysis would not have solved any of the problems, perhaps only made them less visible. The discrepancy between the OSL and other evidence indicates that there is much we still do not understand about these sites or their ages.

8.3. Samples from playas

UW580, from San Jon, sampled from just above a stratum with Paleoindian material, has moderately high over-dispersion. Because this probably reflects mixing, no justification is present for either central or minimum age models. Ages from either are not far apart (11,800 ± 800 yr and 9200 ± 1100 yr, respectively) and both are consistent with the radiocarbon dates of 9300 to 13,500 years from the Paleoindian stratum. The high over-dispersion prevents better resolution at this point. The upper sample, UW579, has very small sample size, but nevertheless, the central age is consistent with the radiocarbon determined on the stratum directly below it.

9. Conclusions

The goals of this investigation were to evaluate the utility of single-grain OSL dating for various sedimentary environments on the Southern High Plains and to provide at least preliminary ages for a number of archaeological sites. We were able to check the OSL results against radiocarbon ages where these were available but other sites lacked secure chronological control.

In terms of comparisons with independent ages, the results were mixed. In some cases the problems may be unique to luminescence dating (error in estimating the dose rate, for example), but in other cases the problems may relate to proper associations of target (age of projectile points) and dated (age of sediment) events, problems that apply to any dating method. In any case, the advantages of multiple dating methods applied at any one site should be obvious.

In both the draw and playa settings, the deposits, including fine-grained marls, proved datable by OSL. The general consistency of these results with independent radiocarbon evidence supports the use of luminescence as a dating tool on the Great Plains. However, there were discrepancies in OSL ages from dune settings, both where independent age control is available, and where OSL ages could only be compared against "ballpark" estimates obtained by cross-dating (though, of course, the cross-dating must be taken with caution). As discussed, these problems may not relate to any intrinsic difficulties with dune deposits, but rather to dose rate complexities and problematic archaeological associations.

This work also highlights some of the advantages of single-grain dating. Single-grain methods, in combination with tests for partial bleaching, are recommended because of the structural information provided by the distributions. This approach allows evaluation of ages that would not be possible with multi-grain aliquots. It also allowed reasonable ages to be obtained for two samples, UW583 (Mustang Springs) and (assuming the cross-dating is reasonable), UW577 (Milnesand), and in turn suggested why some samples (e.g., UW480 [Lubbock Lake]) may not agree with radiocarbon results.

While multi-grain single aliquots may provide higher precision, in some cases such as UW580 (San Jon) such a higher precision would be misleading and unjustified, given the evidence of mixing. Most sample ages from the central age model agreed with independent evidence much better than those from minimum age models. This differs from the findings of Olley et al. [38], who detected on their samples partial bleaching even with aeolian sediments and therefore found better agreement with independent dating evidence using the minimum age model. There were other samples, however, where neither model seemed appropriate.

As for the ages of various Late Paleoindian unfluted projectile points, the results here are only a start. The OSL dates obtained for sediments associated with these unfluted points are all post-Folsom, as they ought to be. And the ages obtained for the Milnesand and Ted Williamson bonebeds are also in keeping with what we would expect, in a general sense. Those from Bedford Ranch were not. In all cases, more and independent dates will obviously be required to resolve the ages of these remains.

Acknowledgements

This work was funded by the National Science Foundation. Shannon Mahan of the U.S. Geological Service assisted with the sample collection and took gamma spectrometry measurements in the field. James H. Mayer of the University of Arizona helped with one portion of the sample collection. Laboratory work was performed in part by M. Aksel Casson and Amber Earley.

References

[1] M.J. Aitken, Thermoluminescence Dating, Academic Press, London, 1985.
[2] M.J. Aitken, An Introduction to Optical Dating, Oxford University Press, Oxford, 1998.
[3] R.M. Bailey, Towards a general kinetic model for optically and thermally stimulated luminescence of quartz, Radiat. Meas. 33 (2001) 17–45.
[4] M.D. Bateman, A.K. Singhvi, C.D. Frederick, Investigations into the potential effects of pedoturbation on luminescence, Radiat. Meas. 22 (2003) 1169–1176.
[5] L. Bøtter-Jensen, E. Bulur, G.A.T. Duller, A.S. Murray, Advances in luminescence instrument systems, Radiat. Meas. 32 (2001) 523–528.

[6] L. Bøtter-Jensen, S.W.S. McKeever, A.G. Wintle, Optically Stimulated Luminescence Dosimetry, Elsevier Science, Amsterdam, 2003.
[7] B. Buchanon, L. Litwinionek, E. Johnson, V.T. Holliday, J.K. Hicks, Renewed investigations at Milnesand and Ted Williamson Paleoindian sites, Curr. Res. Pleistocene 13 (1996) 8–9.
[8] D.A. Bush, J.K. Feathers, Application of OSL dating to anthrosols: a study of the distribution of D_E of quartz through surface and buried soil profiles from Archaic-aged earthen mounds in the SE United States, Quat. Sci. Rev. 22 (2003) 1153–1159.
[9] M.L. Clarke, H.M. Rendell, Late Holocene dune accretion and episodes of persistent drought in the Great Plains of Northeastern Colorado, Quat. Sci. Rev. 22 (2003) 1051–1058.
[10] J.K. Feathers, Single-grain OSL dating of sediments from the Southern High Plains, Quat. Sci. Rev. 22 (2003) 1035–1042.
[11] S.L. Forman, R. Oglesby, R.S. Webb, Temporal and spatial patterns of Holocene dune activity on the Great Plains of North America: megadroughts and climate links, Global and Planetary Change 29 (2001) 1–29.
[12] R.F. Galbraith, R.G. Roberts, G.M. Laslett, H. Yoshida, J.M. Olley, Optical dating of single and multiple grains of quartz from Jinmium rock shelter, northern Australia: Part I, experimental design and statistical models, Archaeometry 41 (1999) 339–364.
[13] R.F. Galbraith, R.G. Roberts, H. Yoshida, Error variation in OSL palaeodose estimates from single aliquots of quartz: a factorial experiment, Radiat. Meas. 39 (2005) 289–307.
[14] C.V. Haynes Jr., Contributions of radiocarbon dating to the geochronology of the peopling of the New World, in: R.E. Taylor, A. Long, R.S. Kra (Eds.), Radiocarbon after Four Decades: an Interdisciplinary Perspective, Springer, New York, 1992, pp. 355–374.
[15] C.V. Haynes Jr., Clovis-Folsom geochronology and climatic change, in: O. Soffer, N.D. Praslov (Eds.), From Kostenki to Clovis: Upper Paleolithic-Paleo-Indian Adaptations, Plenum Press, New York, 1993, pp. 219–236.
[16] M.G. Hill, V.T. Holliday, D.J. Sanford, A further evaluation of the San Jon site, New Mexico, Plains Anthropol. 40 (1995) 369–390.
[17] V.T. Holliday, Holocene soil-geomorphological relationships in a semiarid environment: the Southern High Plains of Texas, in: J. Boardman (Ed.), Soils and Quaternary Landscape Evolution, John Wiley and Sons, London, 1985, pp. 325–357.
[18] V.T. Holliday, The Blackwater Draw Formation (Quaternary): a 1.4-plus m.y. record of eolian sedimentation and soil formation on the Southern High Plains, Geol. Soc. Am. Bull. 101 (1989) 1598–1607.
[19] V.T. Holliday, Late Quaternary stratigraphy of the Southern High Plains, in: E. Johnson (Ed.), Ancient Peoples and Landscapes, Museum of Texas Tech University, Lubbock, 1995, pp. 289–313.
[20] V.T. Holliday, Stratigraphy and Paleoenvironments of the Late Quaternary Valley Fills on the Southern High Plains, 186, Geological Society of America Memoir, Boulder, CO, 1995.
[21] V.T. Holliday, Paleoindian Geoarchaeology of the Southern High Plains, University of Texas Press, Austin, 1997.
[22] V.T. Holliday, Origin and evolution of lunettes on the High Plains of Texas and New Mexico, Quat. Res. 47 (1997) 54–69.
[23] V.T. Holliday, The evolution of Paleoindian geochronology and typology on the Great Plains, Geoarchaeology 15 (2000) 227–290.
[24] V.T. Holliday, Stratigraphy and geochronology of Upper Quaternary Eolian sand on the Southern High Plains of Texas and New Mexico, United States, Geol. Soc. Am. Bull. 113 (2001) 88–108.
[25] V.T. Holliday, S.D. Hovorka, T.C. Gustavson, Lithostratigraphy and geochronology of fills in small playa basins on the Southern High Plains, Geol. Soc. Am. Bull. 108 (1996) 953–965.
[26] V.T. Holliday, E. Johnson, H. Haas, R. Stuckenrath, Radiocarbon ages from the Lubbock Lake site, 1950-1980: framework for cultural and ecological change on the Southern High Plains, Plains Anthropol. 28 (1983) 165–182.
[27] V.T. Holliday, E. Johnson, H. Haas, R. Stuckenrath, Radiocarbon ages from the Lubbock Lake site, 1981-1984, Plains Anthropol. 30 (1985) 277–291.
[28] K. Lepper, N. Agersnap Larsen, S.W.S. McKeever, Equivalent dose distribution analysis of Holocene eolian and fluvial quartz sands from Central Oklahoma, Radiat. Meas. 32 (2000) 603–608.
[29] C.W. Martin, W.C. Johnson, Variation in radiocarbon ages of soil organic matter fractions from late Quaternary buried soils, Quat. Res. 43 (1995) 232–327.
[30] J.A. Matthews, Radiocarbon dating of surface and buried soils: principles, problems and prospects, in: K.S. Richards, R.R. Arnett, S. Ellis (Eds.), Geomorphology and Soils, Allen and Unwin, London, 1985, pp. 269–288.
[31] D.J. Meltzer, Altithermal archaeology and paleoecology at Mustang Springs, on the Southern High Plains of Texas, Am. Antiq. 56 (1991) 236–267.
[32] D.J. Meltzer, Human responses to Middle Holocene (Altithermal) climates on the North American Great Plains, Quat. Res. 52 (1999) 404–416.
[33] D.J. Meltzer, M.B. Collins, Prehistoric water wells on the Southern High Plains: clues to altithermal climate, J. Field Archaeol. 14 (1987) 9–27.
[34] D.R. Muhs, V.T. Holliday, Origin of late Quaternary dune fields on the Southern High Plains of Texas and New Mexico, Geol. Soc. Am. Bull. 113 (2001) 75–87.
[35] A.S. Murray, J.M. Olley, Precision and accuracy in the optically stimulated luminescence dating of sedimentary quartz: a status review, Geochromometria 21 (2002) 1–16.
[36] A.S. Murray, A.G. Wintle, Luminescence dating of quartz using an improved single-aliquot regenerative-dose protocol, Radiat. Meas. 32 (2000) 57–73.
[37] J.M. Olley, G.G. Caitcheon, R.G. Roberts, The origin of dose distributions in fluvial sediments, and the prospect of dating single grains from fluvial deposits using optically stimulated luminescence, Radiat. Meas. 30 (1999) 207–217.
[38] J.M. Olley, T. Pietsch, R.G. Roberts, Optical dating of Holocene sediments from a variety of geomorphic settings using single grains of quartz, Geomorphology 60 (2004) 337–358.
[39] J.R. Prescott, D.J. Huntley, J.T. Hutton, Estimation of equivalent dose in thermoluminescence dating—the *Australian slide* method, Ancient TL 11 (1993) 1–5.
[40] J. Rich, S. Stokes, Optical dating of geoarchaeologically significant sites from the Southern High Plains and South Texas, USA, Quat. Sci. Rev. 20 (2001) 949–959.
[41] F.H.H. Roberts, Archaeological and geological investigations in the San Jon district, eastern New Mexico, Smithsonian Miscellaneous Collections 103(4), Washington, DC, 1942.
[42] E.H. Sellards, Fossil bison and associated artifacts from Milnesand, New Mexico, Amer. Antiq. 20 (1955) 336–344.
[43] F. Sellet, A changing perspective on Paleoindian chronology and typology: a view from the Northern Plains, Arctic Anthropol. 38 (2001) 48–63.
[44] J.S. Singarayer, R.M. Bailey, S. Ward, S. Stokes, Assessing the completeness of optical resetting of quartz OSL in the natural environment, Radiat. Meas. 40 (2005) 13–25.
[45] S. Stokes, D.R. Gaylord, Optical dating of Holocene dune sands in the Ferris dune field, Wyoming, Quat. Res. 39 (1993) 274–281.
[46] S. Stokes, J.B. Swinehart, Middle- and late-Holocene dune reactivation in the Nebraska Sand Hills, USA, Holocene 7 (1997) 263–272.
[47] K.J. Thomsen, A.S. Murray, L. Bøtter-Jensen, Sources of variability in OSL dose measurements using single grains of quartz, Radiat. Meas. 39 (2005) 47–61.
[48] J. Wallinga, On the detection of OSL age overestimation using single-aliquot techniques, Geochronometria 21 (2002) 17–26.
[49] J.M. Warnica, T. Williamson, The Milnesand site—revisited, Am. Antiq. 33 (1968) 16–24.
[50] H.M. Wormington, Ancient Man in North America, Fourth ed., Denver Museum of Natural History, Popular Series 4, Denver, 1957.